Nanotechnology-based treatment for chemotherapy-resistant breast cancer.

Abraham H. Abouzeid[1], Niravkumar R. Patel[1], Ilya M. Rachman[2], Sean Senn[2], and Vladimir P. Torchilin[1]

[1]Department of Pharmaceutical Sciences, Center for Pharmaceutical Biotechnology and Nanomedicine, Northeastern University, Boston, MA, USA and [2]Immix Biopharma Inc, Los Angeles, CA, USA

ABSTRACT

Background: Treatment of metastatic cancer remains a formidable clinical challenge. Better therapeutic options with improved tissue penetration and tumor cell uptake are urgently needed. Targeted nanotherapy, for improved delivery, and combinatory drug administration aimed at inhibiting chemo-resistance may be the solution.

Purpose: The study was performed to evaluate the therapeutic efficacy of polymeric PEG-PE micelles, co-loaded with curcumin (CUR) and doxorubicin (DOX), and targeted with anti-GLUT1 antibody (GLUT1) against MDA-MB-231 human breast adenocarcinoma cells both in vitro and in vivo.

Methods: MDA-MB-231 DOX-resistant cells were treated with non-targeted and GLUT1-targeted CUR and DOX micelles as a single agent or in combination. Tumor cells were also inoculated in female nude mice. Established tumors were treated with the micellar formulations at a dose of 6 mg/kg CUR and 1 mg/kg DOX every 2 d for a total of 7 injections.

Results: CUR+DOX-loaded micelles decorated with GLUT1 had a robust killing effect even at low doses of DOX in vitro. At the doses chosen, non-targeted CUR and CUR+DOX micelles did not exhibit significant tumor inhibition versus control. However, GLUT1-CUR and GLUT1-CUR+DOX micelles showed a significant tumor inhibition effect with an improvement in survival.

Conclusion: We showed a dramatic improvement in efficacy between the non-targeted and GLUT1-targeted formulations both in vitro and in vivo. Also, importantly, the addition of CUR to the micelle, has restored sensitivity to DOX, with resultant tumor growth inhibition. Hence, we confirmed that GLUT1-CUR+DOX micelles are effective in vitro and in vivo and deserve further investigation.

Keyword list

Antibody-targeted nanoparticles, breast carcinoma, chemotherapy-resistance, glucose transporters, GLUT-1, nuclear factor-kappa B (NF-kB)

2. INTRODUCTION

Despite significant improvements in treatment of early stages of cancer, the ability to effectively treat advanced forms of the disease is still hindered by cancer's resistance to chemotherapy, biologics, and radiotherapy. Available evidence points to the nuclear factor-kappa B (NF-κB)-induced cascade of gene expression as being instrumental in producing such chemo- and radiation-resistant tumor phenotypes[1]. Many published studies show correlation between induction and constitutive overexpression of NF-κB and the resistant tumor phenotype in breast[2], colon[3], pancreas[4], and other tissues.

Biosensing and Nanomedicine VII, edited by Hooman Mohseni, Massoud H. Agahi, Manijeh Razeghi,
Proc. of SPIE Vol. 9166, 916606 · © 2014 SPIE · CCC code: 0277-786X/14/$18 · doi: 10.1117/12.2064660

NF-κB upregulates the inhibitory of apoptosis proteins (IAPs) such as COX2, BCL2 and survivin [5] thus promoting tumor proliferation, invasion, and metastasis [6]. Many conventional chemotherapeutic agents, such as doxorubicin (DOX), upregulate NF-κB especially at suboptimal doses[7] and adding curcumin (CUR) helps to blunt this effect. CUR, the principal curcuminoid of the Indian spice turmeric, has shown excellent NF-κB - inhibitory action against many different cancer cell types in vitro[8]. CUR downregulates NF-κB mainly by AKT downregulation and via some other mechanisms as well[5]. The inhibition of NF-κB activation appears to restore cancer cell's sensitivity to chemo- and radiotherapy [9]. The wealth of data supporting CUR's anti-cancer activity led to multiple attempts to use it in human clinical trials. Unfortunately, delivering sufficient quantities of curcumin to cancer cells in vivo has remained a major challenge in clinical oncology[10]. Part of the challenge is the hydrophobic nature of curcumin and its poor oral bioavailability which could be overcome by using drug delivery systems via our targeted delivery systems provide much higher tumor cell uptake of their payloads than untargeted lipid- or polymer-based drug carriers[11]. The present study was designed to test the breast cancer-inhibitory effect of a micelle nanoparticle carrying various combinations of CUR and DOX, and decorated with the anti-GLUT1 antibody (GLUT1) as a tumor-targeting moiety.

Since glucose is a polar molecule and cannot get into the cell via simple diffusion, a family of proteins, SLC2/GLUT, regulates glucose uptake into cells. There are 14 GLUT proteins including the GLUT1 protein[12]. Although the GLUT1 glucose transporter is found in multiple normal tissues, it is significantly overexpressed on many types of tumors[13-16] in order to support cell growth and is thought to contribute significantly to the Warburg effect[17]. In addition, GLUT1 forms the basis for tumor visualization by PET scan with FDG-labeled glucose[18, 19]. Many studies have reported that the overexpression of GLUT1 is a marker of poor prognosis and decrease in survival among variety of cancer types[20-23]. This increased expression of GLUT1 provides a great molecular target for anti-cancer therapeutics.

Our recent work showed excellent efficacy of GLUT1-targeted CUR and DOX-loaded micelles against chemotherapy-resistant colon adenocarcinoma HCT-116 cells in vitro and in vivo[24].

In this study, we investigated the efficacy of the GLUT1-targeted CUR and DOX-loaded micelles against chemo-resistant MDA-MB-231 breast cancer cells. We have found that this CUR/DOX co-loaded polymeric micelles decorated with GLUT1 had a robust tumor killing in MDA-MB-231 cancer cells both in vitro and in nude mice xenografts. These findings point to the general applicability of targeted NF-kB suppression as a therapeutic strategy for treatment of chemo-resistant cancers.

3. MATERIALS AND METHODS

3.1 Materials

1,2-Distearoyl-sn-glycero-3-phosphoethanolamine-N-[methoxy(polyethylene glycol)-2000] (PEG2000–DSPE) was purchased from CordenPharma International (Plankstadt, Germany); 1,2-dioleoyl-sn-glycero-3-phosphoethanolamine (DOPE) was purchased from Avanti Polar Lipids (Alabaster, AL,USA) and used without further purification; pNP-PEG3400-pNP was purchased from Laysan Bio (Arab, AL). Curcumin was purchased from Sigma (St. Louis, MO, USA catalog #C7727). Doxorubicin free base was purchased from US Biological (Swampscott, MA). GLUT1 (C-20) sc-1605 antibody was purchased from Santa Cruz Biotechnology, Inc. (Santa Cruz, CA). CellTiter-blue® was purchased from Promega (Madison, WI). Matrigel™ basement membrane matrix was purchased from BD Biosciences (Bedford, MA). All other reagents and buffer solution components were analytical grade preparations. Distilled and deionized water was used in all experiments.

3.2 Methods

3.2.1 Cell cultures

MDA-MB-231 human colon cancer cells were purchased from ATCC (Manassas, VA) and maintained in McCoy's 5A medium (ATCC 30-2007™) supplemented with 10% heat-inactivated fetal calf serum and 1% penicillin, streptomycin, and amphotericin from Cell-Gro (Kansas City, MO). Cells were maintained at 37 °C in a humidified incubator with 5% CO2, and were passaged according to ATCC protocols.

3.2.2 Preparation of drug-loaded micelles

CUR and/or DOX loaded micelles were prepared by the thin film hydration method. Specific amounts of CUR (3 mg/ml in 0.1% acetic acid methanol stock solution) and/or DOX free base (0.5 mg/ml in methanol stock solution) were added to PEG2000-PE in chloroform. The concentration of the micelle-forming material used in all experiments was 5mM. Organic solvents were removed by rotary evaporation, to form a thin film of drug/micelle –forming component mixture, which was further dried under high vacuum overnight to remove all remaining organic solvents (Freezone 4.5 Freeze Dry System Labconco, Kansas City, MO). Drug-loaded micelles are spontaneously formed when the film is resuspended in a polar solvent, phosphate buffer saline (PBS) pH 7.4 in this case. The mixture was incubated in a water bath at 40°C for 10 min and then vortexed for at least 5 minutes to ensure proper resuspension of the lipid film. Excess non-incorporated drugs were separated by centrifugation (13,500g) for 5 minutes followed by filtration through a sterile 0.2 μm syringe filter before characterization (Nalgene, Rochester, NY).

3.2.3 Preparation of the GLUT1-targeted micelles

To attach the GLUT1 antibody to the micelles, a pNP-PEG3400-PE component was synthesized. The activated p-nitrophenylcarbonyl (pNP) group at the distal end of the PEG3400-PE monomer reacts with amino-groups of various ligands yielding a stable urethane (carbamate) bond. Synthesis of this polymer was performed according to standardized in-lab procedures. Briefly, pNP-PEG3400-pNP and DOPE were dissolved in dry chloroform, co-incubated with TEA and then reacted at RT under argon with continuous stirring overnight. Solvents were then removed by rotary evaporation, and films were further dried under vacuum for at least 4 hours to remove all residual solvents. The dried films were then rehydrated with 0.001M HCl (pH 3.0) and separated on a Sepharose (CL4B) column. Fractions were collected and analyzed by TLC to identify aliquots containing the pNP-PEG3400-PE product; these fractions were then frozen, lyophilized, weighed and reconstituted with chloroform to appropriate stock concentrations, and stored at -80° C for further use.

To attach GLUT1 to micelles, the reactive polymer, pNP–PEG3400–PE in chloroform was placed in a round-bottom flask. Chloroform was evaporated under a rotary evaporator to form a thin film. Films were further dried under vacuum overnight to remove any residual solvents, and rehydrated with stock GLUT1 solution in 1X PBS (pH 7.4) at a molar ratio of pNP-PEG-PE:GLUT1 40:1. The pH of the solution was adjusted with 1.0 N NaOH to 8.5 as needed. Reaction time was 4hrs at RT, to allow sufficient GLUT1 conjugation and complete hydrolysis of unreacted pNP groups at the higher pH. GLUT1-PEG-PE micelles were then dialyzed using a 300,000 MWCO membrane against PBS (pH 7.4) for 1hr followed by another 4hrs of dialysis in PBS (pH 7.4) to ensure the complete removal of unconjugated antibody. Targeted combination micelles were prepared by co-incubating drug-loaded micelles with GLUT1-modified micelles at a ratio of 2 mole% of the reactive polymer, pNP–PEG3400–PE, to PEG2000-PE. Samples were vortexed and allowed to mix for at least 4 hours at room temperature.

Conjugation efficiency of GLUT1 was measured using a micro BCA kit (Pierce, Rockford, IL) according to the manufacture's manual. Protein content was determined by comparing GLUT1-micelles to a known concentration of antibody and BCA standards. Signals from GLUT1 samples were normalized with plain micelle samples at the same lipid concentration. In addition, to verify the preservation of the GLUT1 specific activity after the conjugation with PEG3400-PE and incorporation into micelles, a direct ELISA was used. Briefly,

ELISA plates were coated with 50 μl of 1 μg/ml solution of the GLUT1 blocking peptide and incubated overnight at 4 °C. The plates were then rinsed with PBS containing 0.05% Tween 20 pH 7.4 (PBS-T) and then incubated for 2 hours at 37 °C with 200 μl of PBS-T containing 2 mg/ml casein solution as a blocking buffer to prevent a non-specific binding. The blocking buffer was then discarded, and 50 μl serial dilutions of GLUT1-containing micelles and GLUT1 standards were added and incubated for 1 hour at 37 °C. The plates were extensively washed with PBS-T, and 50 μl of horseradish peroxidase/donkey anti-goat IgG conjugate diluted 5000:1 was added. After 1 hour incubation at 37 °C, the plates were washed thoroughly with PBS-T and bound peroxidase was quantified by adding a 50 μl aliquot of K-blue substrate (Neogen Corp., Lexington, Kentucky, USA) and incubating at room temperature in the dark for 30 min. The intensity of

the color developed was analyzed using an ELISA reader at the wavelength of 492 nm (BioTek, Model: EL 800) and GEN 5.0 software.

3.2.4 Characterization of micelles

3.2.4.1 Micelle size

The micelle size (hydrodynamic diameter) was measured by the dynamic light scattering (DLS) using a N4 Plus Submicron Particle System (Coulter Corporation, Miami, FL, USA). The micelles were diluted with the deionized water until the concentration providing the light scattering intensity between 5x104 and 1x106 counts/second. The particle size distribution of all samples was measured in triplicate.

3.2.4.2 Drug incorporation efficiency

Drug incorporation efficiency was measured by the reverse phase HPLC using an Xbridge C18 (4.6 mm x 250 mm) column (Waters Corporation, Milford, MA) on a Hitachi Elite LaChrome HPLC equipped with an autosampler (Pleasanton, CA) and diode array detector. A gradient method was used with the mobile phase consisting of acetonitrile, water supplemented with 0.2%TFA, and methanol. The flow rate was 1 ml/min. DOX was detected at wavelengths of 254 and 485 nm, while CUR was detected at 420nm. Sample injection volume was kept constant at 50 µl and the sample run time was 20 min. Concentration of drug was determined by measuring the area under the curve of the corresponding peaks. Standard curves of stock drug solution, dissolved in the mobile phase, were used to determine the concentrations of incorporated drugs in micelles. Ten microliters of drug-loaded micelles were diluted in 990 µl of the mobile phase to disrupt the micelles and release the entrapped drug for detection. All samples were analyzed in triplicate. Separation of peaks for both drugs was achieved with DOX and CUR detected at 5.247 and 13.953 min, respectively. The standard curves obtained for DOX and CUR from the HPLC method had an R2 value of 0.999 (n=3). This method was developed to detect DOX and CUR in the same micellar formulation. DOX elutes in the initial stage where the mobile phase is relatively polar; whereas CUR elutes at the later stage of the gradient when the mobile phase is less polar.

3.2.5 Cell viability assays

Viability of cells was measured using the Cell Titer-Blue® (Promega, Madison, WI) viability assay according to the manufacture's protocol. Briefly, cells were seeded in 96-well plates at a density of 3,000 cells/well and grown for 24 hrs. Then cells were incubated with the various formulations for 48 hrs in serum complete medium. After 48 hrs of treatment, the medium was removed and the cells were washed with 200 µl serum complete medium and then incubated with 100 µl medium containing 20 µl Cell Titer-Blue® reagent. Cell viability was then evaluated after 2 hrs of incubation by measuring the fluorescence (excitation 530 nm, emission

590 nm) using Synergy HT multi-detection microplate reader (Biotek, Winooski, VT). PBS-treated cells were taken as controls to calculate % cell viability and the treatment was carried out in triplicate and at least 3 times.

3.2.6 In vivo tumor inhibition study

Six-week-old female NU/NU nude mice were purchased from Charles River Laboratories International Inc. (Needham, MA). MDA-MB-231 cell suspensions (5x106 cells/0.2 mL PBS:Matrigel 1:1 v/v) were injected subcutaneously into the right flank of each mouse. Mice were treated when their tumor volume reached ~150 mm3 15 days after tumor inoculation. Animals were randomly divided into six groups (six animals per group). DOX (1 mg/kg) and CUR (6 mg/kg) were injected i.v. every other day for a total of 7 injections. Tumor volume was estimated from measurements in two perpendicular dimensions taken manually with vernier calipers and applying the formula (L x W2)/2, where L is the longest dimension and W is the dimension perpendicular to L.

3.2.7 Data analysis

Data were generated in multiples of triplicates for proper statistical analysis. In vitro experiments are reported as mean + SD while in vivo experiments are reported as mean + SEM . Comparisons between two groups were made using

Student's t test and with more than two groups, one way ANOVA was used to compare results. Statistical significance was determined by a p-value < 0.05.

4. RESULTS

4.1 Preparation and characterization of micelles

Our overall goals were to prepare and characterize of CUR-, DOX-, and CUR+DOX- loaded micelles untargeted and targeted with the GLUT1 and evaluate their in vitro cytotoxicity against MDA-MB-231 breast carcinoma cells and assess changes in anti-tumor activity with the combination treatment in vivo. CUR and/or DOX drug-loaded micelles were prepared by the thin film hydration method. At 5 mM concentration of PEG2000-PE, we were able to successfully incorporate DOX at a concentration of ~0.45 mg/ml (~3.2 % w/w). CUR was also effectively encapsulated at a concentration of ~1.2 mg/ml (8.5% w/w). The same concentrations of both drugs were achieved when co-loaded into a single micellar formulation. Loading efficiency was not affected by the addition of the targeting moiety. The micelles had sizes of 12.2 + 1.6 nm and a zeta potential of - 29.2 ± 0.91 mV for the untargeted formulations. The GLUT1-targeted micelles had slightly larger size of 19.9 + 2.9 nm and a zeta potential of - 18.9 ± 1.1 mV

A reverse phase HPLC method using a C18 column was developed to determine the drug concentrations in the micellar formulations simultaneously with clear separation between the CUR and DOX peaks. We were able to calculate the loading efficiency which was ~95 % at the conditions used. Antibody activity after the attachment to the distal end of the PEG3400-PE polymer was tested before proceeding with the experiments using the ELISA test with the GLUT1 blocking peptide as the anitgen. The conjugation efficiency of the antibody was ~70% and the activity was retained after conjugation as determined by BCA and ELISA.

4.2 Cell viability assays

The in vitro cytotoxicity of the different micellar formulations was investigated using the MDA-MB-231 cell line. Empty untargeted and GLUT1-targeted PEG–PE micelles had minimal cytotoxic effects on the cells at the corresponding concentrations used.

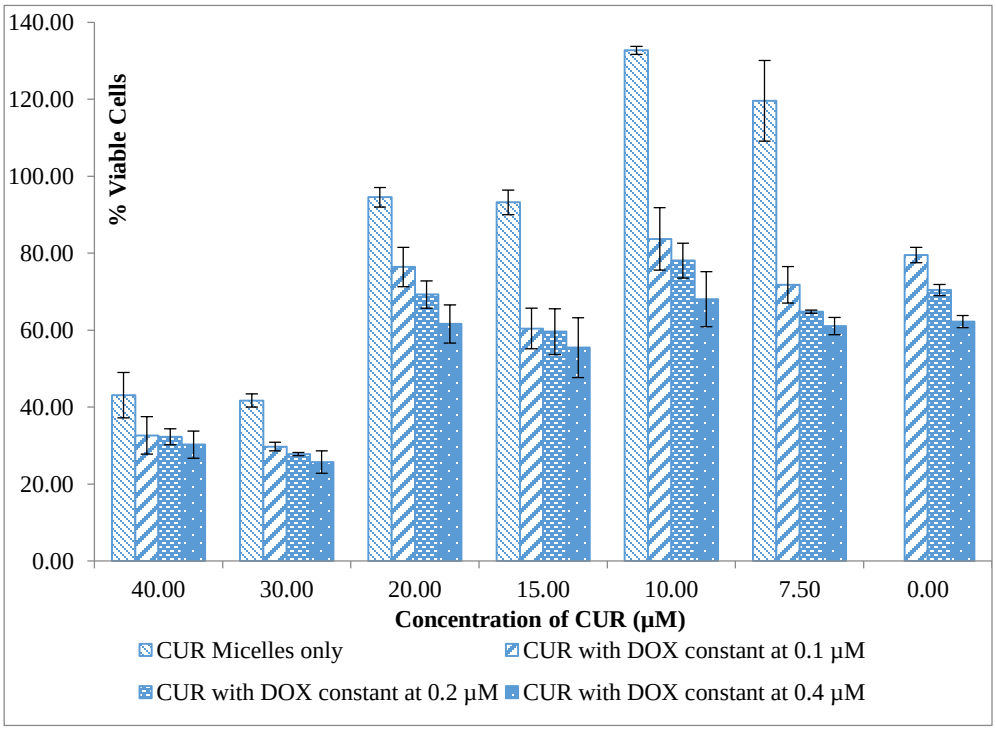

Figure 1: Viability of MDA-MB-231 cells after 48hrs of continuous incubation with combination micelles at various concentrations of CUR and DOX. Cell viability was determined using CellTiter-blue cell viability assay. Data shown are representative of 3 independent experiments and each performed in triplicate.

Figure 1 shows that CUR+DOX-loaded micelles decorated with GLUT1 had a robust killing effect even at low doses of DOX. Greater than 70 % killing of the MDA-MB-231 cells was observed with a low dose of DOX in combination with GLUT1-targeted CUR micelles, as compared to less than 40% with the highest DOX dose alone.

4.3 Tumor inhibition study

Nude mice bearing ~ 150 mm3 MDA-MB-231 tumors were treated with 6 mg/kg CUR and 1 mg/kg DOX as a single treatment or in combination every 2 days for 7 doses. At the doses chosen, the formulations exhibited minimum to no non-specific toxicity in vivo as no significant decrease in body weight was observed throughout the study. Also, GLUT1-CUR+DOX treatment was significantly different from the CUR group.

CUR micelles at a dose of 6 mg/kg and GLUT1-empty micelles did not show any significant tumor growth inhibition versus PBS control group in this study. GLUT1-CUR+DOX group showed statistically significant tumor growth suppression as compared to all other groups.

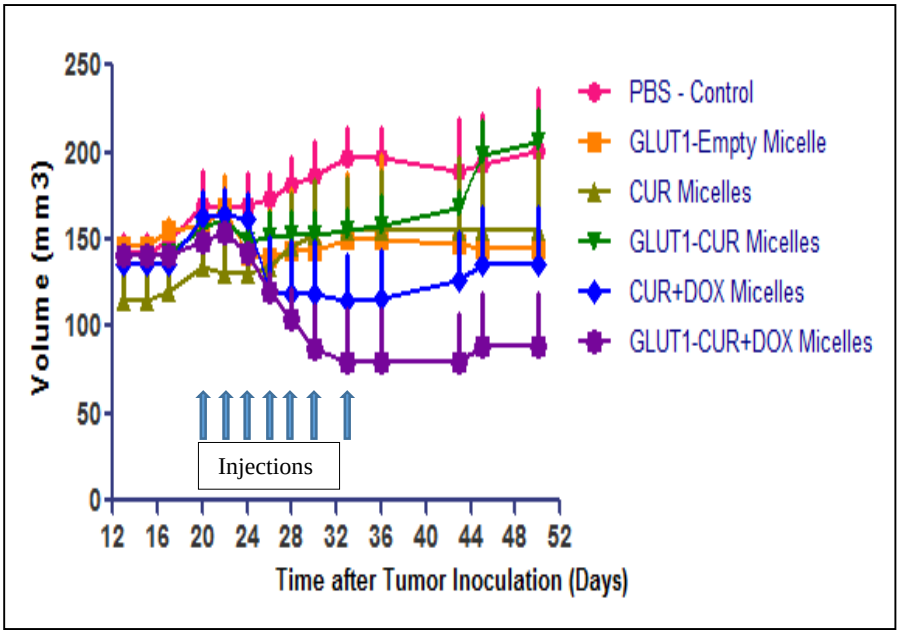

Figure 2: Tumor inhibition studies of various micellar formulations. Nude mice bearing ~150 mm^3 MDA-MB-231 tumors were treated every 2 days starting at Day 20 except last injection administered at day 33 (7 total IV injections) at a dose of 6 mg/kg CUR and 1 mg/kg DOX. N≥6 with SEM.

5. DISCUSSION:

In clinical settings, administration of many cytotoxic chemotherapeutic agents leads to up-regulating of NF-κB, which induces chemo-resistant phenotypes in tumors. To circumvent this phenomenon, clinicians attempt to administer high doses of drugs to achieve tumor lysis, which in turn leads to numerous undesirable side effects. The GLUT1-targeted CUR and DOX-loaded combination micelle could help minimize these side effects and at same time improve the treatment outcome. This could be achieved by increasing drug uptake at the target site by utilizing GLUT1 and at the same time preventing the cancer cells from acquiring drug resistance through the CUR-mediated inhibition of the NF-κB activity. In this study, we administered a suboptimal dose of DOX, and this low dose was unable to confer resistance to the MDA-MB-231 xenografts; this was evident since the GLUT1-CUR+DOX micelles significantly inhibited tumor growth and had dramatic effect on survival. CUR-loaded micelles had negligible effects on tumor growth at the dose chosen; however, due to the increased internalization of targeted micelles via the GLUT1, a significant inhibition of tumor growth was observed by the GLUT1-CUR micelles. We also observed that GLUT1-empty micelles had some effect on tumor growth, although with no statistically significant difference from the PBS-treated control group. Still, this trending could be attributed to the decrease in glucose uptake by blocking the GLUT1 transport protein. GLUT1 is not present in certain normal tissues but due to malignant transformation, it is able to be detected in various peri-necrotic

regions in many human tumor types [25]. This difference in expression between normal tissue and tumors is sufficient to permit the targeting of GLUT1 transporter with minimal side effects.

Here, we have demonstrated the efficiency of using GLUT1 as a targeting moiety and also as a tool to inhibit the GLUT1 transporter leading to a decrease in glucose uptake by colon cancer cells. We also revealed that the polymeric micelles used are suitable for delivering and shielding CUR and DOX in vivo. These results extend the applicability of GLUT1-targeted DOX+CUR micelles to breast cancer model, similar to those observed in our previous study with colon cancer cells. These data further suggest that the present combinatory approach can be a promising novel treatment strategy for chemo-resistant cancers.

6. REFERENCES:

[1]. Samanta, A.K., et al., Overexpression of MEKK3 confers resistance to apoptosis through activation of NFkappaB. J Biol Chem, 279(9): p. 7576-83 (2004)

[2]. Shostak K, C.A., NF-κB, stem cells and breast cancer: the links get stronger. Breast Cancer Research, 13(4): p. 214 (2011)

[3]. Voboril R, W.-V.J., Constitutive NF-kappaB activity in colorectal cancer cells: impact on radiation-induced NF-kappaB activity, radiosensitivity, and apoptosis. Neoplasma, 53(6): p. 518-23. (2006)

[4]. Arlt, A., et al., Role of NF-kappaB and Akt/PI3K in the resistance of pancreatic carcinoma cell lines against gemcitabine-induced cell death. Oncogene, 22(21): p. 3243-51 (2003)

[5]. Gupta, S.C., et al., Inhibiting NF-κB activation by small molecules as a therapeutic strategy. Biochimica et Biophysica Acta (BBA) - Gene Regulatory Mechanisms, 1799(10–12): p. 775-787 (2010)

[6]. Huang S, D.A., Bucana CD, Fidler IJ., Nuclear factor-kappaB activity correlates with growth, angiogenesis, and metastasis of human melanoma cells in nude mice. Clinical Cancer Research, 6(6): p. 2573-81 (2000)

[7]. Yeh, P.Y., et al., Involvement of nuclear transcription factor-κB in low-dose doxorubicin-induced drug resistance of cervical carcinoma cells. Biochem Pharmacol, 66(1): p. 25-33 (2003)

[8]. Anand, P., et al., Curcumin and cancer: An "old-age" disease with an "age-old" solution. Cancer Letters, 267(1): p. 133-164 (2008)

[9]. Chaturvedi, M.M., et al., NF-kappaB addiction and its role in cancer: 'one size does not fit all'. Oncogene, 30(14): p. 1615-30 (2011)

[10]. Epelbaum, R., et al., Curcumin and gemcitabine in patients with advanced pancreatic cancer. Nutr Cancer, 62(8): p. 1137-41 (2010)

[11]. Kirpotin, D.B., et al., Antibody Targeting of Long-Circulating Lipidic Nanoparticles Does Not Increase Tumor Localization but Does Increase Internalization in Animal Models. Cancer Research, 66(13): p. 6732-6740 (2006)

[12]. Mueckler, M. and B. Thorens, The SLC2 (GLUT) family of membrane transporters. Molecular Aspects of Medicine, 34(2–3): p. 121-138 (2013)

[13]. Macheda, M.L., S. Rogers, and J.D. Best, Molecular and cellular regulation of glucose transporter (GLUT) proteins in cancer. J Cell Physiol, 202(3): p. 654-62 (2005)

[14]. Yamamoto, T., et al., Over-expression of facilitative glucose transporter genes in human cancer. Biochemical and Biophysical Research Communications, 170(1): p. 223-230 (1990)

[15]. Boado, R.J., K.L. Black, and W.M. Pardridge, Gene expression of GLUT3 and GLUT1 glucose transporters in human brain tumors. Molecular Brain Research, 27(1): p. 51-57 (1994)

[16]. Brown RS, W.R., Overexpression of Glut-1 glucose transporter in human breast cancer. An immunohistochemical study. Cancer, 72(10): p. 2979-85 (1993)

[17]. Vander Heiden, M.G., L.C. Cantley, and C.B. Thompson, Understanding the Warburg effect: the metabolic requirements of cell proliferation. Science, 324(5930): p. 1029-33 (2009)

[18]. Gu, J., et al., Correlation of GLUT-1 overexpression, tumor size, and depth of invasion with 18F-2-fluoro-2-deoxy-D-glucose uptake by positron emission tomography in colorectal cancer. Dig Dis Sci, 51(12): p. 2198-205 (2006)

[19]. Squires, M.S., et al., Biological characterization of AT7519, a small-molecule inhibitor of cyclin-dependent kinases, in human tumor cell lines. Mol Cancer Ther, 8(2): p. 324-32 (2009)

[20]. Evans, A., et al., Glut-1 as a therapeutic target: increased chemoresistance and HIF-1-independent link with cell turnover is revealed through COMPARE analysis and metabolomic studies. Cancer Chemother Pharmacol, 61(3): p. 377-93 (2008)

[21]. Szablewski, L., Expression of glucose transporters in cancers. Biochimica et Biophysica Acta (BBA) - Reviews on Cancer, 1835(2): p. 164-169 (2013)

[22]. Cantuaria, G., et al., Expression of GLUT-1 glucose transporter in borderline and malignant epithelial tumors of the ovary. Gynecol Oncol, 79(1): p. 33-7 (2000)

[23]. Sung, J.Y., et al., Expression of the GLUT1 glucose transporter and p53 in carcinomas of the pancreatobiliary tract. Pathol Res Pract, 206(1): p. 24-9 (2010)

[24] Abouzeid, A., "Anti-cancer activity of anti-GLUT1 antibody-targeted polymeric micelles co-loaded with curcumin and doxorubicin," J Drug Targeting 21, 994-1000 (2013).

[25]. Airley, R., et al., Glucose transporter Glut-1 is detectable in peri-necrotic regions in many human tumor types but not normal tissues: Study using tissue microarrays. Ann Anat, 192(3): p. 133-8 (2010)